Research Article

Hocine Menana*, Mohamad Farhat, Melika Hinaje, Kevin Berger, Bruno Douine, and Jean Lévêque

Eddy current modeling in linear and nonlinear multifilamentary composite materials

https://doi.org/10.1515/phys-2018-0026
Received Oct 30, 2017; accepted Nov 24, 2017

Abstract: In this work, a numerical model is developed for a rapid computation of eddy currents in composite materials, adaptable for both carbon fiber reinforced polymers (CFRPs) for NDT applications and multifilamentary high temperature superconductive (HTS) tapes for AC loss evaluation. The proposed model is based on an integro-differential formulation in terms of the electric vector potential in the frequency domain. The high anisotropy and the nonlinearity of the considered materials are easily handled in the frequency domain.

Keywords: Eddy current, multifilamentary composite materials, anisotropy, nolinearity, numerical modeling

PACS: 85.25.Am, 84.71.Mn, 74.25.N-, 02.60.Cb, 02.70.Bf

1 Introduction

Electromagnetic field modeling in composite materials such as carbon fiber reinforced polymers (CFRPs) or multifilamentary high-temperature superconductive (HTS) tapes, is in many cases a challenging task. Numerical modeling is then often necessary [1, 2], where the conventional numerical tools have difficulties to provide accurate solutions in reasonable computing times due to multiscale dimensions, nonlinearities and high anisotropies. In these cases, specific modeling approaches meeting a better compromise between accuracy and computing time are needed.

In previous works, we have developed an electromagnetic model, based on an integro-differential formulation, for a rapid eddy current computation in carbon fiber reinforced composite polymers for nondestructive testing (NDT) applications [2]. In this work, this model is extended to model eddy current losses in multifilamentary HTS composite tapes submitted to external sinusoidal time varying magnetic fields. Indeed, both materials have similarities in their geometrical structures, constituted of filaments embedded in a matrix. In the case of CFRPs, the filaments are carbon fibers embedded in a polymer matrix resulting in poor conductivities and high anisotropies, whereas in the HTS tapes, the filaments are made of a nonlinear conductive material (HTS) and the matrix is made of a high conductive material. A numerical scheme is proposed to take into account the nonlinearity of the constitutive law, relating the electrical current density to the electrical field, in the frequency domain rather than in the time domain as it is commonly done. This ensures the stability and the rapidity of convergence of the numerical scheme. The proposed approach is validated by comparison to theoretical and experimental results. For loss computation, it is particularly shown that the nonlinearity of the HTS tapes can be avoided by considering a high anisotropy factor as reported in [3].

The modeled system and the electromagnetic formulation are presented in the next sections. Numerical results and validation are given in the last section.

2 The modeled system

The modeled system (Figure 1) consists of a multifilamentary composite sample of length L_t, width W_t and thickness T_t, constituted of filaments embedded in a matrix. The sample is submitted to an external sinusoidal time varying magnetic flux density ($\vec{B}^a$). The whole system is characterized by the vacuum magnetic permeability (μ_0). To avoid the modeling at the filament scale, a homogenized nonlinear electrical conductivity tensor is defined for the sample, given by (1), where $\sigma_{//}$ and σ_T denote the

***Corresponding Author: Hocine Menana:** Group of Research in Electrical Engineering of Nancy (GREEN), University of Lorraine Vandoeuvre-Lès-Nancy, France; Email: hocine.menana@univ-lorraine.fr
Mohamad Farhat, Melika Hinaje, Kevin Berger, Bruno Douine, Jean Lévêque: Group of Research in Electrical Engineering of Nancy (GREEN), University of Lorraine Vandoeuvre-Lès-Nancy, France

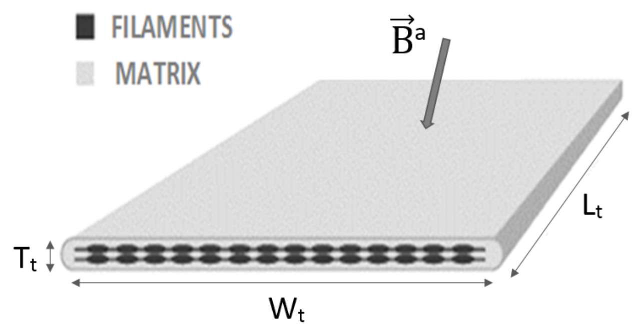

Figure 1: The modeled system

conductivities parallel and transverse to the filaments [2–4].

$$\bar{\bar{\sigma}} = diag\ (\sigma_{//},\ \sigma_T\ ,\ \sigma_T), \tag{1}$$

For the CFRPs, the matrix is a non-conductive material and the transverse conductivity depends essentially on the volume fraction of the carbon filaments. In the case of HTS tapes, the transverse conductivity depends on both the filaments volume fraction (η_s) and shape, the matrix conductivity (σ_m), the interface between the filaments and matrix, and the source filed orientation [4, 5]. The longitudinal conductivity depends mainly on the filaments volume fraction as given in (2), where, $E_{//}$ and $J_{//}$ are respectively the components of the electric field and current density parallel to the filament orientation.

$$\sigma_{//} = \eta_s J_{//} E_{//}^{-1} + (1 - \eta_s)\sigma_m \tag{2}$$

The CFRPs are characterized by linear electromagnetic properties, whereas, HTS tapes are characterized by a nonlinear conductivity tensor. In this work, the nonlinearity is reported only on $\sigma_{//}$. The power law is used to express the nonlinear constitutive law between the components of the electric field and current density parallel to the filament direction, given by (3), where E_c is a characteristic electric field usually set to $1\mu V/cm$, and J_c is the critical value of the electric current density. The power exponent (n) characterizes the steepness of the transition shape from the superconducting to the normal state.

$$E_{//} = E_c \left[J_{//} J_c^{-1} \right]^n \tag{3}$$

The critical value of the electric current density depends in its turn on the magnetic flux density ($\vec{B}$). The Kim's law is used to take into account this dependence, as given in (4), where J_{c0} is the critical current density at zero magnetic field, and $B_0$is a characteristic magnetic flux density [6]:

$$J_c(B) = J_{c0} \left[1 + \left\| \vec{B} \right\| B_0^{-1} \right]^{-1} \tag{4}$$

3 Model formulation and implementation

Starting from the electrical current conservation, we derive the latter as the curl of the electric vector potential (T):

$$\vec{\nabla}.\vec{J} = 0 \ \Leftrightarrow\ \vec{J} = \vec{\nabla} \times \vec{T} \tag{5}$$

Considering that the magnetic field varies sinusoidally with time, from the Maxwell-Faraday law in the frequency domain, with the angular frequency ω, we have:

$$\vec{\nabla} \times \overline{\overline{\sigma^{-1}}}\ \vec{\nabla} \times \vec{T} = -i\omega\, \vec{B} \tag{6}$$

We separate the magnetic flux density into its source and reaction terms, evaluated by integral equations (7) involving the source ($\vec{J}_S$) and the eddy currents. In (7) $\vec{B}^a$ is an externally applied magnetic flux density satisfying$\vec{\nabla}.\vec{B}^a = 0$.

$$\vec{B}(\vec{r}) = \frac{\mu_0}{4\pi} \int_{\Omega} \frac{[\vec{\nabla}' \times \vec{T}(r') + \vec{J}_S] \times (\vec{r} - \vec{r}')}{\left|\vec{r} - \vec{r}'\right|^3}\, dv + \vec{B}^a(\vec{r}) \tag{7}$$

In the following, to compact the expressions of the formulas, the matrix writing is adopted, where $\bar{\bar{C}}$, $\bar{\bar{R}}$ and $\bar{\bar{M}}$ are respectively the curl, the resistivity and the integral matrices. Equation (7) can thus be rewritten as follows:

$$\overline{B} = \overline{B}^a + \mu_0 \bar{\bar{M}} \overline{J}_S + \mu_0 \bar{\bar{M}}\, \bar{\bar{C}}\, \overline{T} \tag{8}$$

Introducing (7) in (6), we obtain the flowing integro-differential equation:

$$\bar{\bar{C}}\, \bar{\bar{R}}\, \bar{\bar{C}}\, \overline{T} = -i\omega\ (\overline{B}^s + \mu_0 \bar{\bar{M}}\, \bar{\bar{C}}\, \overline{T}) \tag{9}$$

The integral part of the formulation allows a direct interaction between the system elements, and thus only the active parts of the system are discretized. The finite difference method is used to discretize the curl operator. The matrix equation (9) is solved iteratively which allows to take into account the nonlinearity of the resistivity matrix as shown in the flowchart described in Figure 2. We start by solving (9) by considering only the source term of the magnetic flux density, then we evaluate the eddy currents, after that we evaluate the reaction term of the magnetic flux density; at this step, we actualize the value of the critical current density, then we actualize the conductivity tensor and solve again the equation (9) with the actualized values of the magnetic flux density and the conductivity tensor. The operation is repeated until convergence. An iterative method (conjugate gradient method) is used to solve the matrix equation. As the source term is divergence free, no gage condition is needed as shown by Z. Ren in [7].

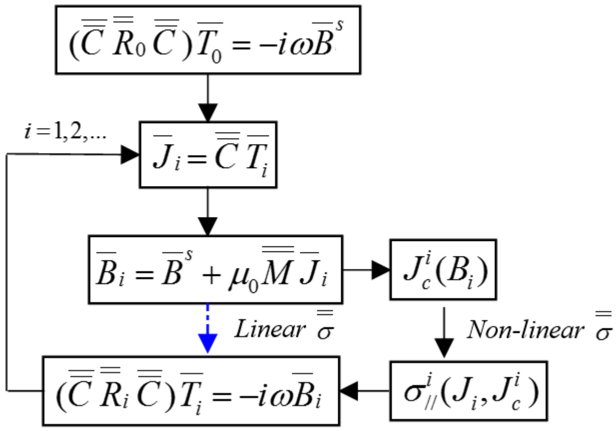

Figure 2: Iterative solving procedure

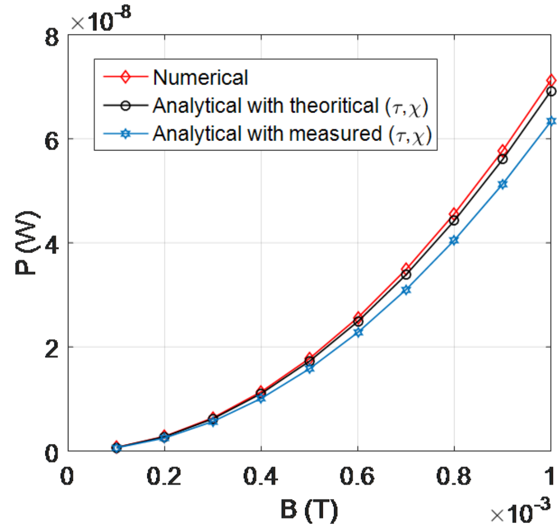

Figure 3: Comparison between the numerical and analytical results of the eddy current losses

4 Numerical examples and validation

In this section a numerical example is considered for validation purpose. We consider an HTS multifilamentary untwisted tape submitted to an external magnetic field oriented normal to its large surface (width). The results of the eddy current losses are compared to coupling losses (Q_c) given by the Campbell's model [8], expressed as J/m^3/cycle in (10), involving a time constant of the magnetic flux penetration (τ) and a geometrical factor (χ) related to the demagnetizing factor [9].

$$Q_c = \frac{B^{a2}}{2\mu_0}\left[2\pi\chi\frac{\omega\tau}{1+\omega^2\tau^2}\right] \tag{10}$$

$$\begin{cases} \chi = \frac{\pi W_t}{4T_t} \\ \tau = \frac{{L_t}^2\sigma_m\mu_0}{\pi^2\chi} \end{cases} \tag{11}$$

The system specifications are given in Table 1. For the comparison, we use in (10) both theoretical and experimental values of the parameters (τ, χ). The experimental ones are given by D. Zola *et al.*, obtained through measurements for the specified geometry [9].

Table 1: Used parameters

Symbol	Quantity	Value
W_t | T_t | L_t	Tape dimensions	3.2mm | 0.25mm | 6.5mm
η_s	HTS volume fraction	0.32
σ_m | σ_T	Matrix and transverse conductivities	6.3 10^7 Sm^{-1} | 8.210^7 Sm^{-1}
J_{C0} | B_0 | n	Typical quantities	9.65 10^7 Am^{-2} | 0.3T | 15
χ | τ	Measured values of the geometrical factor and time constant [9]	9.8 | 0.32 ms

Figure 3 shows a comparison between the analytical and numerical results of the eddy current losses. The comparison is performed in the limits of the validity of the analytical model (feeble fields) [8, 9]. The results present constant discrepancy over the entire interval of calculation between the numerical and analytical values, which is of 2.8% when theoretical values of the parameters (τ, χ) are used and about 11% when the measured ones are used. This discrepancy is due to errors in both models. Indeed, in the analytical model, the tape is considered isotropic and the dependence of the critical current on the magnetic field is not taken into account. The magnetic field is also assumed to be homogeneously distributed on the tape, which is not really satisfied as it can be shown in Figure 4 through the eddy current repartition in the tape reflecting a spatial variation of the magnetic field. Moreover, the measured parameters used in the analytical model have been determined experimentally with a certain precision. In the other hand, the numerical model is also based on some assumptions, in particular, the use of an homogenized conductivity tensor, and present a certain numerical error. In particular, the transverse conductivity is calculated simply by increasing the conductivity of the matrix by the volume fraction of the superconductor, *i.e.*, $\sigma_T = (1+\eta_s)\sigma_m$, and may thus be overestimated.

In our investigations, we were also interested in verifying a result presented by G.B.J Mulder *et al.* announcing that the behavior of a multifilamentary HTS tape become similar to that of an anisotropic material as the anisotropy

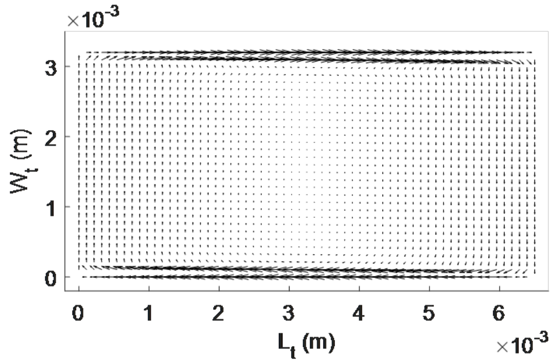

Figure 4: Eddy currents repartition in the tape

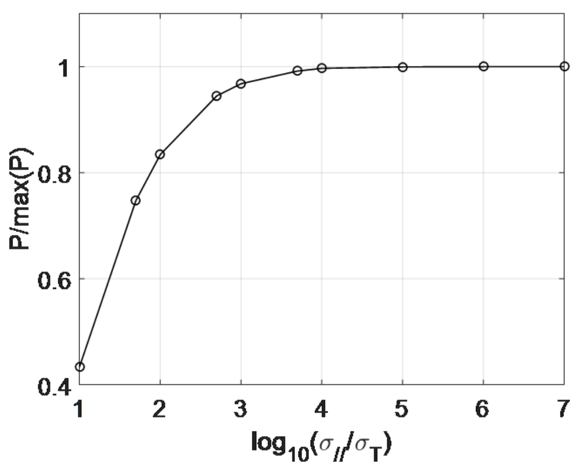

Figure 5: Variation of the eddy current losses according to the anisotropy factor (B^s = 1T, Pmax = 0.19W)

increases [3], with less assumptions by considering the magnetic reaction of the tape, which was ignored in the work presented by G.B.J Mulder *et al.* At this end, we have considered a linear $\sigma_{//}$ in (1). Figure 5 represents the normalized variation of the eddy current losses with respect to the anisotropy factor (ratio between $\sigma_{//}$ and σ_T). It is interesting to notice that the eddy current losses become constant beyond an anisotropy factor of about 10^4which confirms the results reported by G.B.J Mulder *et al.*

Figure 6 represents the variation of the eddy current losses according to the applied magnetic flux density for three cases: linear anisotropic conductivity ($\sigma_{//} = 10^4\sigma_T$) and nonlinear anisotropic conductivity ($\sigma_{//}(J) \neq \sigma_T$) with and without taking account of the variation of $J_c(B)$. An agreement is shown between the results corresponding to the constant value of the longitudinal conductivity and those corresponding to the case where it depends only on the electrical current density. The results corresponding to

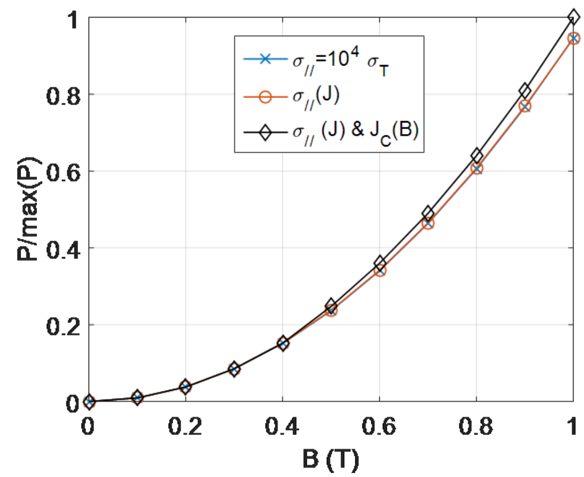

Figure 6: Variation of the normalized eddy current losses according to the applied magnetic flux density for three cases: anisotropic linear conductivity ($\sigma_{//} = 10^4\sigma_T$) and anisotropic nonlinear conductivity ($\sigma_{//}(J)$) with and without considering $J_c(B)$

the case where the longitudinal conductivity depends on both the current and magnetic flux densities show a little discrepancy with the others results, presenting a greater power loss for the high values of the applied magnetic flux density, due to the decrease of the value of the longitudinal conductivity. For feeble values of the applied magnetic flux density, one can thus neglect the variations of $\sigma_{//}(J)$ and $J_c(B)$, considering only an anisotropic linear conductivity ($\sigma_{//} = 10^4\sigma_T$).

5 Conclusions

In this work, we have extended a model developed in a previous work for eddy current modeling in carbon fiber reinforced polymers (CFRPs) to model eddy current losses in multifilamentary high-temperature superconductive (HTS) tapes using the geometrical and physical similarities between these two materials constituted of filaments embedded in a matrix, characterized by multiscale dimensions, nonlinearities and high anisotropies.

Considering sinusoidal time varying magnetic fields, the problem is solved iteratively, taking account of the nonlinearity of the constitutive laws, in the frequency domain rather than in the time domain as it is commonly done, resulting in a considerable gain in computation time. Moreover, it was shown that, for low values of the applied magnetic flux densities, one can consider the HTS tape as a high anisotropic linear conductor.

The model is tested on a simple geometry for validation purpose, but it is intended to be used for complex geometries. In future works, it will be interesting to test new numerical schemes for the discretization of the formulation, such as the degenerated hexahedral Whitney elementsin a finite element scheme as presented in [10].

References

[1] Grilli F., Numerical modeling of HTS applications, IEEE Transactions on Applied Superconductivity, 2016, 26, 0500408.

[2] Menana H., Féliachi M., An integro-differential model for 3D eddy current computation in CFRPs, IEEE Transactions on Magnetics, 2011, 47, 756-763.

[3] Mulder G.B.J., Niessen E.M.J., Coupling losses of multifilamentary superconductors having several concentric regions and mixed matrix, IEEE Transactions on Applied Superconductivity, 1993, 3, 142-145.

[4] Oomen M.P., AC loss in superconducting tapes and cables, PhD thesis, Twente University, Enschede - Netherlands, 2000.

[5] Amemiya N., Enomoto N., and Shirai S., FEM analysis of AC loss in twisted Bi-2223 multifilamentary tapes carrying AC transport current in AC transverse magnetic field with arbitrary orientation, IEEE Transactions on Applied Superconductivity, 2004, 14, 782-785.

[6] Douine B., Berger K., Lévêque J., Improvement of Jc(b) determination method using the virgin magnetization curve for HTS, Proceedings of the 23th International Conference on Magnet Technology - MT23, (14 - 19 Jul 2013, Boston, United States), Boston, 2013.

[7] Ren Z., Influence of the R.H.S. on the convergence behavior of the curl-curl equation, IEEE Transactions on Magnetics, 1996, 32, 665–658.

[8] Campbell A.M., A general treatment of losses in multifilamentary superconductors, Cryogenics, 1982, 22, 3-16.

[9] Zola D., Gömöry F., Polichetti M., Strýček F., Seiler E., Hušek I. et al., A study of coupling loss on bi-columnar BSCCO/Ag tapes through ac susceptibility measurements, Supercond. Science and Technology, 2004, 17, 501-511.

[10] Bui H.K., Wasselynck G., Trichet D., Berthiau G., Degenerated Hexahedral Whitney Elements for Electromagnetic Fields Computation in Multi-Layer Anisotropic Thin Regions, IEEE Transactions on Magnetics, 2016, 52, 7208104.